

# The Effects of Impact Vibration on Peripheral Blood Vessels and Nerves

Kristine M. KRAJNAK<sup>1\*</sup>, Stacey WAUGH<sup>1</sup>, Claud JOHNSON<sup>1</sup>, G. Roger MILLER<sup>1</sup>,  
Xueyan XU<sup>1</sup>, Christopher WARREN<sup>1</sup> and Ren G. DONG<sup>1</sup>

<sup>1</sup>Engineering and Controls Technology Branch, National Institutes for Occupational Safety and Health, USA

Received November 17, 2012 and accepted July 30, 2013

Published online in J-STAGE September 27, 2013

**Abstract:** Research regarding the risk of developing hand-arm vibration syndrome after exposure to impact vibration has produced conflicting results. This study used an established animal model of vibration-induced dysfunction to determine how exposure to impact vibration affects peripheral blood vessels and nerves. The tails of male rats were exposed to a single bout of impact vibration (15 min exposure, at a dominant frequency of 30 Hz and an unweighted acceleration of approximately 345 m/s<sup>2</sup>) generated by a riveting hammer. Responsiveness of the ventral tail artery to adrenoreceptor-mediated vasoconstriction and acetylcholine-mediated re-dilation was measured *ex vivo*. Ventral tail nerves and nerve endings in the skin were assessed using morphological and immunohistochemical techniques. Impact vibration did not alter vascular responsiveness to any factors or affect trunk nerves. However, 4 days following exposure there was an increase in protein-gene product (PGP) 9.5 staining around hair follicles. A single exposure to impact vibration, with the exposure characteristics described above, affects peripheral nerves but not blood vessels.

**Key words:** Vibration, Cardiovascular disorders, Musculoskeletal disorders, Sensorineural disorders, Animal model

## Introduction

Repetitive exposure to hand-transmitted vibration through the use of powered hand tools has been associated with the development of a disorder referred to as hand-arm vibration syndrome (HAVS). The hallmark symptom of HAVS is cold-induced vasospasms that result in finger and hand blanching. However, workers with HAVS also display a loss of tactile sensitivity in the hands and fingers, pain, reductions in manual dexterity and grip strength, joint injuries and muscle atrophy<sup>1, 2</sup>. Although the duration of the exposure appears to be the primary factor associated with the development of HAVS, a number of

other factors including the dominant exposure frequency intensity (i.e., acceleration), also contribute to the risk of developing the disorder<sup>2</sup>.

The precise exposure-response relationship between vibration frequency and the risk of developing HAVS has still not been determined. Although recent studies indicate that frequencies in the range of 60–300 Hz may increase the risk of vascular and sensorineural symptoms that are part of HAVS, the current ISO 5349-1<sup>3</sup> standard developed by the International Standards Organization (ISO), presents a frequency-weighting curve that gives the greatest weighting to low-frequency vibration (i.e., less than 16 Hz), and the weighting factor dramatically decreases at frequencies greater than 30 Hz. There also is some controversy regarding the risk of developing peripheral vascular and sensorineural symptoms and the use of impact tools (e.g. riveting hammers, impact wrenches, jackleg drills).

\*To whom correspondence should be addressed.  
E-mail: ksk1@cdc.gov

Impact tools emit a dominant frequency that is fairly low (i.e., drive frequency, approximately 30 Hz<sup>8</sup>). However, they also display a cyclic shock (or impact) component that contains a high frequency component (i.e., greater than 1,000 Hz). Some studies examining the effects of impact vibration demonstrate that users of impact tools display an increased risk of developing the symptoms associated with HAVS, but others find no association between exposure and negative health consequences in workers using impact tools<sup>4-7</sup>. Thus, based on the available data and the ISO standard, it is difficult to determine what the risk of developing vascular and sensorineural symptoms is for workers using impact tools.

Animal models have been used to examine the effects of vibration frequency on changes in peripheral vascular and sensorineural function (reviewed in<sup>9</sup>). A rat-tail model was recently developed for assessing the effects of impact vibration on peripheral nerves and sensory function. Govinda Raju *et al.*<sup>10</sup> examined heat sensitivity and changes in nerve ending and nerve trunk morphology in the tails of rats that were exposed to a single bout of vibration generated using a riveting gun. This study found that 4 days following a single exposure to impact vibration, there was a reduction in heat sensitivity in the tail, disruption of the myelin sheath in the nerve trunk and a reduction in protein-gene product (PGP) 9.5 immunostaining in the tail skin that the authors interpreted as a loss of nerve endings. However, the authors did not assess the effects of impact vibration on peripheral vascular physiology or morphology to determine if there were changes that could result in vascular dysfunction. The primary goal of this study was to use a similar model to assess the effects of a single exposure to impact vibration on vascular physiology. Our lab has demonstrated that a single exposure to sinusoidal vibration at 125 Hz results in an increased sensitivity to  $\alpha$ 2C-adrenoreceptor-mediated vasoconstriction and a reduction in endothelial-mediated (i.e. acetylcholine; ACh) re-dilation<sup>11, 12</sup>. These methods were used to assess the effects of a single exposure to impact vibration on vascular function. We also assessed changes in nerve ending and nerve trunk morphology in an additional study.

## Methods

### Animals

Male Sprague-Dawley [Hla: (SD) CVF rats; 6 wk of age at arrival; Hilltop Lab Animals, Inc., Scottdale, PA; body weights 310–320 g ( $\pm$  3.2)] were used in this study. Rats were maintained in a colony room with a 12:12 light:dark

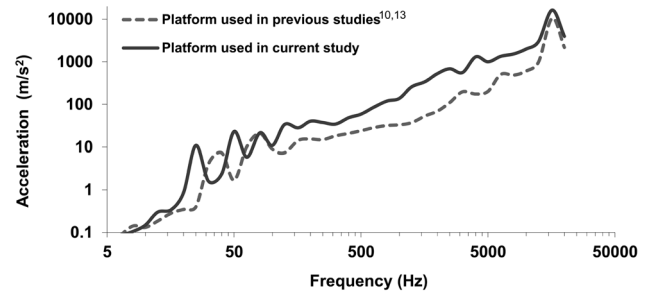


Fig. 1. Comparison of the vibration spectrum measured on the platform used in the current study and that measured on the platform used in the study reported by Govinda Raju *et al.*<sup>10, 13</sup>.

cycle (lights on 0700 h) with Teklad 2918 rodent diet and tap water available *ad libitum*, at the National Institute for Occupational Safety and Health (NIOSH) facility, which is accredited by the Association for Assessment and Accreditation of Laboratory Animal Care International (AAALAC). Rats were allowed to acclimate to the laboratory for one week prior to beginning the study. All procedures were approved by the NIOSH Animal Care and Use Committee and were in compliance with the Public Health Service Policy on Humane Care and Use of Laboratory Animals and the NIH Guide for the Care and Use of Laboratory Animals.

### Vibration exposures

The equipment and protocol were similar to that described by Govinda Raju *et al.*<sup>10, 13</sup>. Rats (n=8/group) were restrained in Broome style restrainers and placed on a non-vibrating platform housed in a sound-attenuating chamber. The sound-attenuating chamber kept noise levels to approximately 60 dB during the exposure. A metal platform was attached to a Honsa riveting hammer (model HTO 13; Milan, IL) that was mounted in a steel frame (frame and platform were identical to those described in<sup>10, 13</sup>). Using procedures similar to those performed in a reported study<sup>13</sup>, the vibration spectrum on the platform was measured with a laser vibrometer. As shown in Fig. 1, the measured vibration spectrum was similar to, but generally higher than that of the platform used in the previous studies<sup>10, 13</sup>. The frequency-weighted acceleration (from 6.3 to 1,250 Hz) was approximately 13 m/s<sup>2</sup> (or approximately 127 m/s<sup>2</sup> unweighted based on the analyses of the full spectrum). The weighted acceleration in the region used for biological analyses was 14 m/s<sup>2</sup> rms (weighted) or 345 m/s<sup>2</sup> rms unweighted. For 15 minutes exposure, the corresponding A (8)-value is 2.3 m/s<sup>2</sup>, which is below the recommended daily exposure action value (2.5

m/s<sup>2</sup>)<sup>3</sup>). The maximum peak acceleration was more than 12,000 m/s<sup>2</sup> at 16 kHz. During exposures, the tails of restrained rats were secured to the platform using Soft-tape (Neurotron Inc., Baltimore, MD, USA)<sup>13</sup>). For peripheral vascular studies, 2 control groups were used; one group was treated in a manner identical to the vibration-exposed rats except their tails were secured to a platform and the rivet gun was not turned on. These rats were exposed to control conditions at the same time rats were exposed to impact vibration, so this group also was exposed to the noise generated by the riveting hammer (even though the noise was attenuated as it was for vibration-exposed rats). However, because previous work has demonstrated that noise-stress has significant effects on peripheral vascular responses<sup>14–16</sup>), a second restraint-control group also was used. These rats had their tails secured to platforms, but they were not exposed to the noise of the riveter. All exposures were performed between 900 and 1,000 h, and were 15 min in length. Rats were returned to the colony room immediately following the exposure.

#### *Reagents*

All chemicals and drugs used in these studies were obtained from Sigma Chemicals (St Louis, MO, USA) unless otherwise noted.

#### *Vascular physiology studies*

Rats used for vascular physiology studies (n=8/group) were anesthetized using pentobarbital (100 mg/mg, i.p.) and euthanized by exsanguination 24 h after vibration or restraint exposure. We chose this time point because we have demonstrated that exposure to sinusoidal vibration has significant effects on ACh-mediated re-dilation<sup>11</sup>) at this time point. Ventral tail arteries from approximately the C12–20 region were dissected, and segments from the proximal section (approximately C13–15) were used to measure vasoconstriction induced by the  $\alpha$ -2C-adrenoreceptor agonist, UK-14304. The distal segment (approximately C16–18) was used to assess vasoconstriction in response to the  $\alpha$ -1 adrenoreceptor agonist, phenylephrine (PE) and re-dilation in response to ACh. Re-dilation after constriction was assessed because ventral tail arteries exhibit little endogenous basal tone<sup>17</sup>). To assess responses to vasoconstricting and dilating factors, artery segments were mounted on pipettes in a microvessel chamber (Living Systems, Burlington, VT, USA) containing HEPEs buffer with glucose (10%) and sodium bicarbonate (chamber buffer)<sup>12</sup>) and maintained at 37°C. Arteries were pressurized to 60 mmHg and allowed to

equilibrate for at least 1 h. The chamber buffer was then changed, and vasoconstricting factors were added in half-log increments. Vasoconstricting and redilating reagents were dissolved in chamber buffer immediately prior to use and were applied directly into the chamber. Changes in the internal diameters of arteries were measured when arteries stabilized (approximately 5 min between applications of the agent) using a XC-ST30 video camera mounted onto a Nikon T1-SM inverted microscope, a video dimension analyzer (Living systems) and Data-Q Instruments software (Akron, OH, USA). Re-dilation in response to ACh applied in half-log increments was measured in PE-constricted arteries, and changes in the internal diameter were measured as described above. Dose-response curves to the various vasoactive factors were generated by averaging dose-dependent responses within a group and using GraphPad (Prism 5.1; San Diego, CA, USA) to generate dose-response curves.

#### *Nerve ending and ventral tail nerve tissue preparation*

To characterize the effects a bout of impact vibration has on peripheral nerves, rats were exposed to a single bout of impact vibration or restraint control conditions (n=6/group), and were euthanized (exsanguinated under pentobarbital anesthesia as described above) 4 d following the exposure. A no-noise control group was not used for this portion of the study because there is little evidence that noise has effects on morphology of nerve endings in the skin. A tail segment from the C16–20 region was dissected. The dissected segment was submersion-fixed in 4% paraformaldehyde for 2 h. This tissue was rinsed in 0.01 M phosphate-buffered saline (PBS), and the skin and a more proximal segment of the tail ventral tail nerve was dissected, placed in molds containing OTC Compound (Tissue Tek, Torrance, CA, USA) and frozen at –80 °C. The ventral portion of the tail nerve was embedded in JB4 for thin sectioning using a previously published procedure and the manufacturer's protocol<sup>18</sup>).

#### *Tail nerve trunk morphology*

Cross-sections (5  $\mu$ m) of JB4-embedded tail nerves were taken on a microtome and mounted on slides as previously described<sup>18</sup>). One slide from each rat was stained with Sudan Black B and another slide was stained with Toluidine Blue using previously published protocols<sup>18</sup>). To assess the density of myelin staining, nerve sections were visualized using an Olympus microscope at a 100  $\times$  oil objective. The center of the section was located, and 3 images from different sections were taken using a SPOT

Flex Mosaic camera and SPOT Advanced Software (version 4.6.4.6/4.6.5.2, Diagnostic Instruments Inc., Sterling Heights, MI, USA). All nerve fibers surrounded by Sudan Black were counted. Images also were loaded into ImageJ (National Institutes of Health, Bethesda, MD, USA), a single threshold was set, and densitometry was used to measure the density and area stained with Sudan Black. The number of myelinated axons, and the 3 area and density measures from each rat were averaged and these averages were used for statistical analyses. An additional set of sections stained with Toluidine Blue were used for mast cell counts and to assess mast cell degranulation. The total number of mast cells was counted in nerve trunks sections (6 sections/rat) and this number was used for statistical analyses.

Immunohistochemistry (IHC) for albumin was performed on sections obtained from frozen nerve trunks. Sections (10  $\mu\text{m}$ ) were cut in a cryostat, thaw-mounted onto slides and stored at  $-20^{\circ}\text{C}$  until processed for albumin IHC using a previously published protocol<sup>19</sup>. The primary antibody, rabbit anti-albumin (Santa Cruz Biotech Inc., Santa Cruz, CA, USA), was used at a final dilution of 1:67, and the secondary antibody was Cy3-labeled donkey anti-rabbit IgG (Jackson Immuno Research Labs, West Grove, PA, USA) used at a final dilution of 1:500. All antibodies were diluted in PBS containing 0.4% Triton-x 100. Nerve sections (3–4 section/ animal, 100  $\mu\text{m}$  between consecutive sections) were centered under the objective, and images from the middle of each nerve section were captured using a Zeiss LSM510 confocal microscope at a final magnification of 45X and ZEN software (Zeiss International, Inc., Thornwood, NY, USA). ImageJ software was used to measure the density of albumin staining in each image. A threshold was set and the area of each image that was above threshold was measured. Because the percent area stained incorporates both the density of the staining (density of staining/area of measurement) this measure was used for analyses.

#### *IHC on skin sections*

Cross-sections (40  $\mu\text{m}$  thick) from frozen skin samples were cut on a cryostat, placed in PBS and stored at  $-4^{\circ}\text{C}$  until processed for IHC. Six separate sets of sections were made for each animal. Each set contained 5 sections, and each section in a set was separated by 200  $\mu\text{m}$ . IHC was performed on a single set of free-floating sections taken from each animal using a slightly modified version of a published protocol<sup>10</sup>. Briefly, sections were rinsed in PBS, incubated in 0.3% hydrogen peroxide in methanol for

30 min and rinsed in PBS. Sections were then incubated in primary antibody diluted in PBS plus 0.3% Triton-x 100 and 10% normal serum (PBS-Tx) at  $4^{\circ}\text{C}$  with mild agitation. PGP9.5 was used to identify nerves, but it was reported that this antibody may also label Langerhans' cells<sup>10</sup>. To differentiate nerve terminal labeling from Langerhans' cell labeling in the skin, an OX-6 antibody as was used as reported in Govinda Raju *et al.*<sup>10</sup>. The primary antibodies used were mouse anti-PGP 9.5 (final dilution 1:1200 MCA-BH7, EnCor Biotechnology Inc., Gainesville, FL, USA) and mouse anti-OX-6 (1:80 MCA46R, AbD Serotec, Raleigh, NC, USA). For PGP9.5 and OX-6 sections were incubated overnight in primary antibody at  $4^{\circ}\text{C}$  with agitation. Sections were then rinsed in PBS and incubated in Cy3-labeled donkey IgG (Jackson Immunolabs, West Grove, PA, USA) used at a final dilution of 1:500 diluted in PBS in Triton-x100, mounted onto slides and air dried. Cover-slips were applied and secured with Prolong Gold (Life Technologies Corporation, Carlsbad, CA, USA). Images were collected on a Zeiss LSM510 confocal microscope and images were collected at the same depth from each sample using a  $10\times$  air objective. Four images were collected at the same depth to ensure that the hair follicles from each sample had similar properties. Photos were imported into ImageJ and defined boxes were made to identify regions around hair follicles and regions just below the dermis. Threshold levels were set and the density and % area stained were quantified using densitometry as described above and previously<sup>18</sup>, and the % area measure was used for analyses.

#### *Statistics*

Data were in the form of percentages, and thus were analyzed to assured they met all assumptions for parametric statistics. Dose-dependent changes in the internal diameter of arteries in response to the application of vasoactive factors were analyzed using 2-way (condition x dose) repeated-measure ANOVAS. Morphological and immunohistochemical data were analyzed using Student's *t*-tests. All analyses were performed using JMP 10.0.0 (2012 SAS Institute Incorporated, Cary NC, USA).

## **Results**

#### *Vascular physiology*

Exposure to impact vibration or the noise of the tool did not result in a difference in baseline diameters of ventral tail arteries (means  $\pm$  SEM; no noise control  $344.14 \pm 6.77$ , noise restraint control  $344.42 \pm 18.65$ , impact  $356.85 \pm$

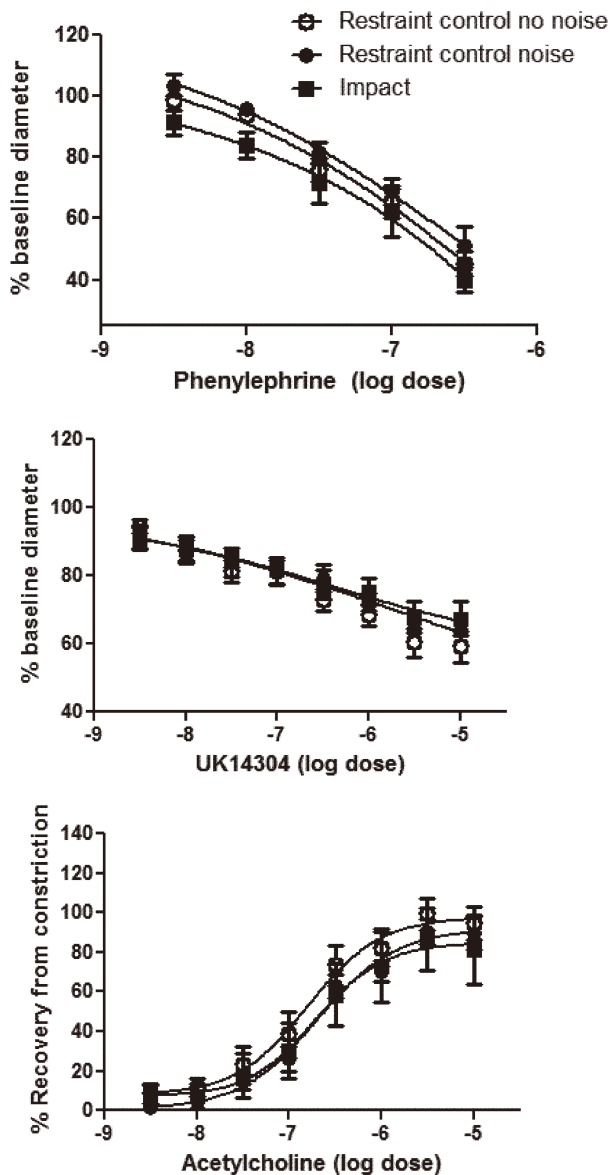


Fig. 2. Dose-dependent vasoconstriction of the ventral tail artery in response to the  $\alpha_1$ - and  $\alpha_2$ -adrenoreceptor agonists phenylephrine (A) and UK14304 (B) was not affected by exposure to impact vibration or noise from the riveting gun. Acetylcholine-induced redilation (C) also was not altered by these exposures. Data are expressed as mean changes (i.e., % constriction from baseline or % redilation from constricted baseline  $\pm$  SEM).

14.64) or dose dependent responses to PE, UK14304 or ACh (Fig. 2).

#### Tail nerve trunk morphology

Inspection of sections containing nerve trunks did not reveal any obvious changes in ventral tail nerve morphology (Fig. 3A). There was no apparent edema (i.e., change in albumin staining), nerve degeneration, disruption of the

myelin sheath, or change in mast cell number. The number of nerve fibers with Sudan Black-stained myelin was not different between the two groups (mean  $\pm$  SEM; control  $185.33 \pm 12.71$ , impact  $191 \pm 9.41$ ). The area stained with Sudan Black was not different between the groups (Fig. 3B). There was also no significant difference between the groups in the area stained with albumin (Fig. 4A), indicating that there was little or no edema induced by the exposure. Although it appears that rats exposed to impact vibration had fewer mast cells than restraint control rats, this difference was not statistically significant (Fig. 4B;  $t(22)=1.76$ ,  $p=0.09$ ). Very little degranulation was seen in any of the sections and therefore not quantified.

#### Skin IHC

The photomicrographs in Fig. 5A show PGP 9.5 immunostaining in the skin of restraint-control and impact exposed rats. Immunolabeling was prevalent around the hair follicles in rats from both groups. There was also labeling throughout the section, including the area just under the dermis, but this labeling was less prevalent. The area from which density measures were collected were similar in both groups (mean  $\pm$  sem: area under the dermis control  $357.9 \pm 28.9$  and vibrated  $362 \pm 3.04$ ; and around the follicle; control  $623.0 \pm 74.62 \mu\text{m}^2$ , vibrated  $613.5 \pm 47.79 \mu\text{m}^2$ ). Analyses of the percent areas stained for PGP9.5 around the hair follicles revealed that the area of staining was significantly greater in impact exposed than control rats (Fig. 5B). Although the % area labeled with PGP9.5 under the dermis also appeared to be somewhat higher in impact-exposed compared to control rats, the difference was not significant (Fig. 5C). Exposure to impact did not affect OX-6 immunostaining around the hair follicles indicating that differences in PGP9.5 immunostaining in this region were not the result of changes in Langhrens' cells (Fig. 5D).

#### Discussion

Repetitive exposure to vibration has been shown to induce peripheral vascular injury and nerve dysfunction in the hands and fingers. However, based on epidemiological studies<sup>4-7</sup>, it is unclear if and how exposure to impact vibration contributes to the development of these disorders. This study used an animal model of impact vibration to assess the effects of an acute exposure on vascular function and peripheral nerve morphology. We found that a single exposure to impact vibration did not affect vascular responsiveness to vasoconstricting or vasodilating factors



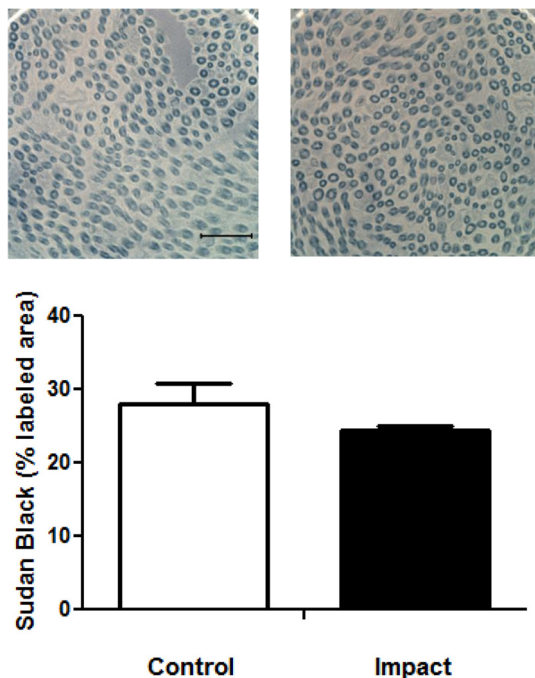


Fig. 3. Representative photomicrographs of Sudan Black B stained nerve sections taken from the ventral tail nerves of restraint control and impact vibration exposed rats (A: bar=10  $\mu$ m). Exposure to impact vibration did not affect percent area stained with Sudan Black (B).

but induced an increase in PGP9.5 staining in peripheral nerve endings around the hair follicles.

Our laboratory previously demonstrated that 24 h after exposure to a single bout of sinusoidal vibration at 125 Hz and a constant, unweighted acceleration of 49  $m/s^2$  r.m.s. There was a reduced sensitivity to ACh-induced redilation of the ventral tail artery and that this change in vascular responsiveness is associated with an increase in vascular hydrogen peroxide levels and a reduction in nitric oxide synthase<sup>12</sup>). In addition, other studies have demonstrated that acute exposure to sinusoidal vibration results in endothelial cell damage<sup>20</sup>) and an increased sensitivity to  $\alpha$ 2C-adrenoreceptor-mediated vasoconstriction in ventral tail arteries<sup>17</sup>). However, exposure to impact vibration did not affect  $\alpha$ 1- or  $\alpha$ 2C-mediated vasoconstriction or ACh-mediated re-dilation. Other studies have also demonstrated that exposure to noise generated by the use of vibrating tools can affect vascular responses in workers<sup>21, 22</sup>), so we also examined vascular responsiveness in rats exposed to restraint and noise from the riveting gun and rats that were exposed to restraint but no noise (restraint-controls with and without noise, respectively). We did not find any differences in vascular responsiveness to vasoconstricting or

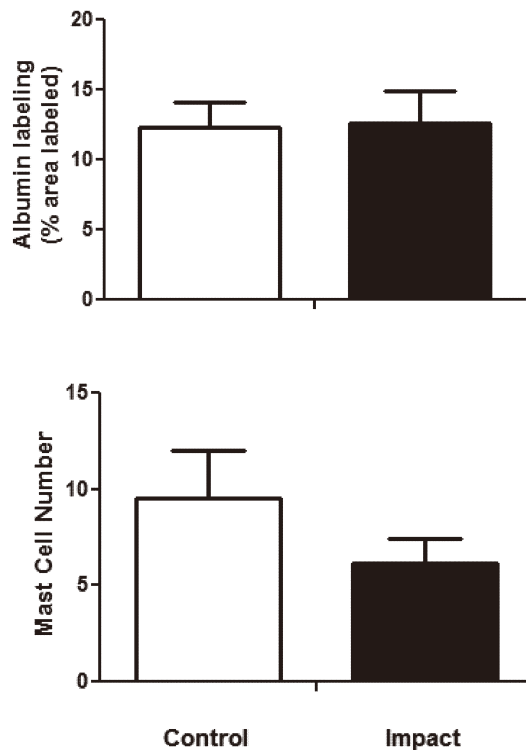


Fig. 4. The percent area immunolabeled with albumin (A) and the number of mast cells stained with Toluidine Blue (B) in ventral tail nerves were not different in control vs. impact exposed rats.

dilating agents between these two groups either, indicating that the potential stress induced by restraint was not increased by noise exposure.

The failure to find an effect of impact vibration on vascular function may be due to a number of factors. First, the exposure durations in these studies were different; the 125 Hz exposure was for 4 h while the impact exposure was for only 15 min. The choice of exposure durations in the study examining sinusoidal vibration was based upon what the maximum daily exposure a worker using a tool with a dominant frequency of 125 Hz should be exposed to<sup>3</sup>). The exposure duration for this study was similar to the exposure duration used in the Govinda Raju study<sup>10</sup>), and they found that a single exposure of a similar duration (i.e., 12 min) affected peripheral nerve morphology. Thus, peripheral nerves may be more sensitive to impact-vibration exposure.

The second difference between the studies was the dominant frequencies to which the tissues of the tail were exposed. Experiments in humans and animals<sup>18, 19</sup>) examining the relationship between vibration frequency and injury have shown that exposures that generate the greatest

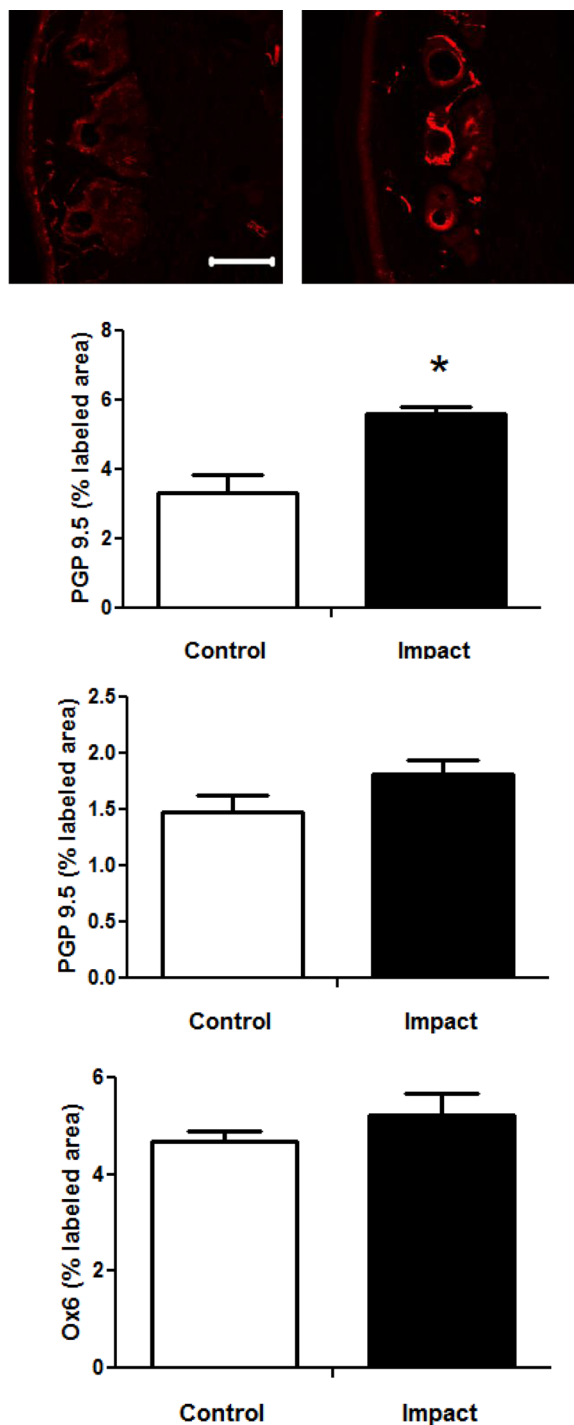


Fig. 5. Representative photomicrographs of PGP9.5 immunostaining in the tail skin from control and impact exposed rats (A; bar=100  $\mu$ m). The box in the control photo is representative of the box used to collect staining measures under the dermis and the box in the impact photo is representative of the box used to collect staining measures around hair follicles. The percent area labeled with PGP 9.5 was greater in impact-exposed than control rats around the hair follicles (B; \* $p < 0.05$ ), but not under the dermis (C). Exposure to impact did not alter the percent area labeled Ox6 around the hair follicles (D).

stress on tissues are more likely to be associated with tissue and physiological responses that precede or are indicative of vascular and peripheral nerve dysfunction<sup>18, 19, 23</sup>. We demonstrated that vibration transmissibility to the tissues of the tail was greatest with exposure to frequencies between 100–300 Hz<sup>24</sup>. This is also the frequency range that appears to induce the greatest stress on the tissues of the fingers<sup>25, 26</sup>. However, as shown in Fig 1, the dominant frequency of the riveting hammer was around 30 Hz. However, a large part of the frequency spectrum was also comprised of frequencies greater than 100 Hz, and these higher frequencies could contribute to the development of an injury or dysfunction. In addition, the acceleration on the rivet platform was about 345  $m/s^2$ . In contrast, the magnitude of sinusoidal vibration used in our previous study was 49  $m/s^2$ ,<sup>12</sup>). Although the magnitudes of the vibrations tend to increase with increasing frequencies, they can only be effectively transmitted to the superficial skin in contact with the platform and they do not penetrate into the deeper layers of the tissue<sup>26</sup>). Hence, the tissue stress and strain in the deep area of the rat tail induced by the platform vibration was likely to be less than that induced by the sinusoidal vibration and thus may not have been severe enough to induce changes in vascular responses.

A recent study demonstrated that an acute exposure to impact vibration resulted in morphological changes in myelination in the nerve trunk and reductions in PGP9.5 immunostaining in nerve fibers in the skin and around the hair follicles in the tails 4 d following vibration exposure<sup>10</sup>). These anatomical changes were associated with reductions in heat sensitivity. Because we did not see changes in vascular function, we examined the effects of a single exposure to impact vibration on peripheral nerve morphology 4 days following the exposure<sup>10</sup>). Acute exposure to impact vibration did not result in a change in the number of myelinated axons, the density of myelin staining or albumin staining in this study. We also did not see any apparent changes in myelin morphology that would indicate that there was damage or injury to myelinated axons in the nerve trunk. To assess the number of axons and density and condition of myelinated fibers, we used Sudan Black staining. Sudan Black stains lipids and is often used to identify myelinated axons<sup>27–29</sup>). Using a stereological-like sampling method and densitometry, we did not find any changes in the density of staining between the different groups. We also did not see any obvious signs of myelin disruption, degeneration or looping. Thus, exposure to impact did not have any effects on myelination of nerve trunk axons on the tail of this study. Govinda Raju

*et al.*<sup>10)</sup> used Toluidine Blue to assess myelin morphology and mast number and degranulation. Although this stain has also been used to identify myelinated axons, Sudan Black is more specific<sup>29)</sup>.

Differences in morphological findings also may be due to the location from which the nerve trunk samples were collected. Our study collected tissue from a region of the tail that was on the platform while the Govinda Raju<sup>10)</sup> study collected tissue from a more proximal region that may have been near the edge of the platform. Tissue near the edge of the platform may experience more bending stress and this could potentially induce more injury. We chose to look at nerve samples from a more distal region so that we could determine the effects of vibration and impact without the additional confounding that could take place because of bending at the edge. These differences in exposure/injury may also account for the fact that we saw very few mast cells or de-granulated mast cells in toluidine stained section.

There were also conflicting findings in PGP9.5 staining results between the two studies. Govinda Raju *et al.*<sup>10)</sup> found that there was a reduction in staining around the nerve endings located near hair follicles and at the surface of the skin 4 d following exposure to impact vibration and the change in staining along with reported changes in nerve ending morphology were interpreted as nerve ending degeneration. In this study, exposure to impact vibration resulted in an increase in PGP9.5 staining around the hair follicles and no changes in the skin. We also didn't see any obvious changes in morphology. The changes in PGP9.5 staining in both studies were not associated with changes in the staining of OX-6 suggesting that the differences in PGP9.5 were not due to the effects of vibration exposure on Langerhen cells<sup>10)</sup>.

PGP9.5 (also known as ubiquitin carboxy-terminal hydrolase L1) is an enzyme that is part of the ubiquitin pathway and it is involved in the breakdown and recycling of proteins<sup>30)</sup>. Immunohistochemical labeling of tissue with PGP9.5 antibodies has been used to identify nerve fibers in peripheral and central nervous system tissue. However, the density and number of labeled nerve fibers appears to be dependent upon the denervation/re-innervation status of nerves; both increases and decreases in immunolabeling have been reported after nerve injury<sup>30-32)</sup>. The same antibody and methods were used to identify PGP9.5 in this study and the study by Govinda Raju<sup>10)</sup>, and thus it is unlikely that the differences in staining were due to these factors. However, as previously mentioned, the location from which samples were collected was different, and

therefore it is possible that the labeled nerves in these two studies sustained different types of injuries and were at different states in the re-innervation/denervation process. Thus, the results from these studies are not necessarily conflicting. However, because PGP9.5 is an enzyme and levels can change depending on the status of nerves, it may not be the best marker to use to assess nerve number or damage/injury after a single exposure to impact vibration, or after such a brief recovery period.

In conclusion, exposure to a single bout of impact vibration had minimal effects on vascular physiology or nerve trunk morphology. We did find changes in PGP9.5 immunostaining of nerve endings in tail skin, but it is unclear if these changes were an indicator of injury/dysfunction or an adaptive response to vibration. There are reports of workers that use impact tools developing HAVS, but these workers have usually been exposed to impact vibration for years<sup>5, 6)</sup>. In addition, occupational exposures in humans can be affected by the grip force used to hold the tool, posture and temperature<sup>8)</sup>. Additional studies assessing the effects of greater intensity vibration, longer duration and repetitive exposures, along with the effectiveness of anti-vibration materials, applied pressure, and temperature may also be performed in animal models. These data may provide some insight as to the contribution of impact vibration to development of vascular and sensorineural symptoms associated with HAVS and to mechanisms underlying the development of these disorders in humans.

## References

- 1) Bernard BP (1997) Hand-Arm Vibration Syndrome. In: Musculoskeletal Disorders and Workplace Factors A critical review of epidemiological evidence for work-related musculoskeletal disorders of the neck, upper extremity, and low back 5c1-31, US Department of Health and Human Services, National Institute for Occupational Safety and Health Cincinnati.
- 2) Griffin MJ, Bovenzi M (2002) The diagnosis of disorders caused by hand-transmitted vibration: Southampton Workshop 2000. *Int Arch Occup Environ Health* **75**, 1-5. [[Medline](#)]
- 3) ISO 5349-1 (2001). Mechanical vibration—Measurement and evaluation of human exposure to hand-transmitted vibration—Part 1: General requirements. International Organization for Standardization, Geneva.
- 4) Aiba Y, Ohshiba S, Ishizuka H, Sakamoto K, Morioka I, Miyashita K, Iwata H (1999) A study on the effects of countermeasures for vibrating tool workers using an impact wrench. *Ind Health* **37**, 426-31. [[Medline](#)] [[CrossRef](#)]
- 5) Burdorf A, Monster A (1991) Exposure to vibration and



- self-reported health complaints of riveters in the aircraft industry. *Ann Occup Hyg* **35**, 287–98. [[Medline](#)] [[CrossRef](#)]
- 6) Musson Y, Burdorf A, van Drimmelen D (1989) Exposure to shock and vibration and symptoms in workers using impact power tools. *Ann Occup Hyg* **33**, 85–96. [[Medline](#)] [[CrossRef](#)]
  - 7) Pelmeur PL, Wills M (1997) Impact vibration and hand-arm vibration syndrome. *J Occup Environ Med* **39**, 1092–6. [[Medline](#)] [[CrossRef](#)]
  - 8) Griffin MJ (1990) *Handbook of Human Vibration*. Academic Press, San Diego.
  - 9) Krajnak K, Riley DA, Wu J, McDowell TW, Welcome DE, Xu XS, Dong RG (2012) Frequency-dependent effects of vibration on physiological systems: experiments. *Ind Health* **50**, 343–53. [[Medline](#)] [[CrossRef](#)]
  - 10) Raju SG, Rogness O, Persson M, Bain J, Riley D (2011) Vibration from a riveting hammer causes severe nerve damage in the rat tail model. *Muscle Nerve* **44**, 795–804. [[Medline](#)] [[CrossRef](#)]
  - 11) Hughes JM, Wirth O, Krajnak K, Miller R, Flavahan S, Berkowitz DE, Welcome DE, Flavahan NA (2009) Increased oxidant activity mediates vascular dysfunction in vibration injury. *J Pharmacol Exp Ther* **328**, 223–30. [[Medline](#)] [[CrossRef](#)]
  - 12) Krajnak K, Waugh S, Johnson C, Miller R, Kiedrowski M (2009) Vibration disrupts vascular function in a model of metabolic syndrome. *Ind Health* **47**, 533–42. [[Medline](#)] [[CrossRef](#)]
  - 13) Xu XS, Riley DA, Persson M, Welcome DE, Krajnak K, Wu JZ, Raju SR, Dong RG (2011) Evaluation of anti-vibration effectiveness of glove materials using an animal model. *Biomed Mater Eng* **21**, 193–211. [[Medline](#)]
  - 14) Matoba T, Ishitake T (1990) Cardiovascular reflexes during vibration stress. *Kurume Med J* **37**, S61–71. [[Medline](#)] [[CrossRef](#)]
  - 15) Pyykko I, Hyvarinen J (1976) Vibration induced changes of sympathetic vasomotor tone. *Acta Chirurgica Scandinavica* **465** (Suppl): 23–6.
  - 16) Solecki L (1995) Effect of impulse vibration and noise on vasomotor function of peripheral blood vessels among pneumatic forge hammer operators. *Cent Eur J Public Health* **3**, 88–9. [[Medline](#)]
  - 17) Krajnak K, Dong RG, Flavahan S, Welcome DE, Flavahan NA (2006) Acute vibration increases  $\alpha_2$ -adrenergic smooth muscle constriction and alters thermosensitivity of cutaneous arteries. *J Appl Physiol* **100**, 1230–7. [[Medline](#)] [[CrossRef](#)]
  - 18) Krajnak K, Miller GR, Waugh S, Johnson C, Li S, Kashon ML (2010) Characterization of frequency-dependent response of the vascular system to repetitive vibration. *J Occup Environ Med* **52**, 584–94. [[Medline](#)] [[CrossRef](#)]
  - 19) Krajnak K, Miller GR, Johnson C, Waugh S, Kashon ML (2012) Frequency-dependent effects of vibration on peripheral nerves and sensory nerve function in a rat model of hand-arm vibration syndrome. *J Occup Environ Med* **54**, 1010–6. [[Medline](#)] [[CrossRef](#)]
  - 20) Curry BD, Govindaraju SR, Bain JL, Zhang LL, Yan JG, Matloub HS, Riley DA (2005) Evidence for frequency-dependent arterial damage in vibrated rat tails. *Anat Rec A Discov Mol Cell Evol Biol* **284**, 511–21. [[Medline](#)] [[CrossRef](#)]
  - 21) Harada N, Iwamoto M, Hirokawa I, Nakamoto M, Sobhan F, Morie T, Kosiyama Y (1995) Response to psychological stressors in hand-arm vibration syndrome patients. *Cent Eur J Public Health* **3** (Suppl): 54–6. [[Medline](#)]
  - 22) Pyykko I (1974) A physiological study of the vasoconstrictor reflex in traumatic vasospastic disease. *Work Environ Health* **11**, 170–86.
  - 23) Dong RG, Welcome DE, McDowell TW, Wu JZ (2004) Biodynamic response of human fingers in a power grip subjected to a random vibration. *J Biomech Eng* **126**, 447–57. [[Medline](#)] [[CrossRef](#)]
  - 24) Welcome DE, Krajnak K, Kashon ML, Dong RG (2008) An investigation on the biodynamic foundation of a rat tail model. *J Eng Med (Proc Instn Mech Engrs, Part H)* **222**: 1127–1141.
  - 25) Dong RG, McDowell TW, Welcome DE (2005) Biodynamic response at the palm of the human hand subjected to a random vibration. *Ind Health* **43**, 241–55. [[Medline](#)] [[CrossRef](#)]
  - 26) Wu JZ, Krajnak K, Welcome DE, Dong RG (2006) Analysis of the dynamic strains in a fingertip exposed to vibration: correlation to the mechanical stimuli on mechanoreceptors. *J Biomech* **39**, 2445–56. [[Medline](#)] [[CrossRef](#)]
  - 27) Cavanagh JB, Passingham RJ, Vogt JA (1964) Staining of Sensory and Motor Nerves in Muscles with Sudan Black B. *J Path Bacteriol* **88**: 89–92.
  - 28) Goyal RK, Sengupta A (1986) A rapid silver-free method for staining the myenteric plexus. *Stain Technol* **61**, 127–34. [[Medline](#)]
  - 29) Cerri PS, Sasso-Cerri E (2003) Staining methods applied to glycol methacrylate embedded tissue sections. *Micron* **34**, 365–72. [[Medline](#)] [[CrossRef](#)]
  - 30) Hurst-Kennedy J, Chin LS, Li L (2012) Ubiquitin C-Terminal Hydrolase L1 in Tumorigenesis. *Biochem Res Int* (in press).
  - 31) Ikeuchi M, Wang Q, Izumi M, Tani T (2012) Nociceptive sensory innervation of the posterior cruciate ligament in osteoarthritic knees. *Arch Orthop Trauma Surg* **132**, 891–895.
  - 32) Ramieri G, Stella M, Calcagni M, Cellino G, Panzica GC (1995) An immunohistochemical study on cutaneous sensory receptors after chronic median nerve compression in man. *Acta Anat (Basel)* **152**, 224–9. [[Medline](#)] [[CrossRef](#)]